Proceedings of the Institution of Civil Engineers
Engineering and Computational Mechanics 161
March 2008 Issue EM1
Pages 17–25
doi: 10.1680/eacm.2008.161.1.17

Paper 700008
Received 17/11/2007
Accepted 05/03/2008

Keywords: dams, barrages & reservoirs/hydraulics & hydrodynamics/water supply

Hubert Chanson
Professor of Civil Engineering, University of Queensland, Brisbane, Australia

ice
Institution of Civil Engineers

The known unknowns of hydraulic engineering

H. Chanson ME, PhD, DEng, EurIng, MIEAust

Hydraulic engineers and researchers deal with the scientific challenges presented by turbulent flow and its interactions with the surroundings. Turbulent flows are characterised by unpredictable behaviour, and, as yet, little systematic research has been conducted in natural systems. This paper discusses the implications of recent developments in affordable instrumentation, which was previously characterised by intrinsic weaknesses that adversely affected the quality of the signal outputs. A challenging application is the unsteady turbulence field in tidal bores. The interactions between open channel flows and movable boundaries and the atmosphere illustrate another aspect of our limited knowledge. Rapid siltation of reservoirs and air entrainment in turbulent free-surface flows are discussed. In both applications, hydraulic engineers require some broad-based expertise. In turn, the education of future hydraulic engineers is of vital importance.

1. INTRODUCTION

Hydraulic engineering involves the science and application of water motion, encompassing the interactions between the flowing fluid and its surroundings. Hydraulic engineers were at the forefront of scientific developments in ancient times. For example, Fig. 1 shows the Roman aqueduct at Gier, which was equipped with several large inverted siphon structures (Fig. 1(b)) of which we know very little.[1–4]

The sheer complexity of hydraulic engineering is closely linked with

(*a*) the wide range of relevant length scales, from a few millimetres for the wall region of a turbulent boundary layer to over 1000 km for the length of a major river
(*b*) the broad range of timescales, from less than 0·1 s at the turbulent dissipation scale to about 10^8 s for reservoir siltation
(*c*) the huge variability of river flows
(*d*) the non-linearity of the basic governing equations.

In rivers, the extreme flow rates may range from zero in drought periods to enormous discharges during floods. For example, the maximum observed flood discharge of the Amazon river at Obidos is about 370 000 m^3/s.[5] Even arid, desert regions are influenced by fluvial action when periodic floodwaters surge down dry watercourses; subsequently, the dry river course returns to being a natural habitat until the next flood occurs.

In this study, it is argued that the 21st century faces scientific challenges in hydraulic engineering that centred on turbulence

(a)

(b)

Fig. 1. The Roman aqueduct at Gier on 8 February 2004. The aqueduct was about 86 km long, and supplied the Roman city of Lugdunum (today Lyon, France); the maximum discharge capacity was up to 0·17 m^3/s (15 000 m^3/day). (a) Elevated channel and arcades du Plat de l'Air at Chaponost. The arcades are 55 m long and up to 15 m high, and include 92 arches. Flow direction is from right to left. The internal channel (*specus*) is visible at the middle top right of the photograph. (b) Inverted siphon structure of Beaunant downstream of the arcades du Plat de l'Air, looking upstream at the 270 m long bridge supporting the pipes. The masonry structure supported 11 (or 12) lead pipes (exterior dia. 230 mm, interior dia. approx. 162 mm). The maximum drop in elevation was 122 m, and the total length of the siphon was 2660 m

and turbulent mixing, and on the interactions between open channel flows and their surroundings.

2. TURBULENCE IN OPEN CHANNEL FLOWS

Predictions of turbulence and turbulent mixing in hydraulic engineering can rarely be accurate without exhaustive field data for calibration and validation. In natural systems, the flow Reynolds number Re is typically within the range 10^5 to 10^8 or more; $Re = \rho V D_H/\mu$, where ρ is the water density, V is the flow velocity, D_H is the equivalent pipe diameter, and μ is the dynamic viscosity. The turbulent flow is characterised by unpredictable behaviour associated with strong momentum exchanges. In his classic experiment, Osborne Reynolds (1842–1912) illustrated this key feature with the rapid mixing of dye in a turbulent flow.[6] Interestingly, Reynolds[7] himself studied basic hydraulic engineering, and the modelling of rivers and estuaries.

Relatively little systematic research has been conducted into the characteristics of turbulence in natural open channels. Most field measurements have been conducted for short periods, or in bursts, sometimes at low frequency, and the data often lack spatial and temporal resolution. However

> Turbulence is a three-dimensional time-dependent motion in which vortex stretching causes velocity fluctuations to spread to all wavelengths between a minimum determined by viscous forces and a maximum determined by the boundary conditions of the flow.[8]

Turbulence measurements must be conducted at high frequency to characterise the small eddies and the viscous dissipation process. They must also be performed over a period significantly longer than the characteristic time of the largest vortical structures, to capture the random nature of the flow and its deviations from Gaussian statistical properties, both of which are key turbulent features.

Turbulence in open channels is neither homogeneous nor isotropic. A basic characteristic is the Reynolds stress tensor. The Reynolds stress is a transport effect that results from turbulent motion induced by velocity fluctuations, with a subsequent increase of momentum exchange and of mixing.[9] The turbulent stress tensor includes normal and tangential stresses, although there is no fundamental difference between the normal stress and the tangential stress. For example, $(\boldsymbol{v}_x + \boldsymbol{v}_y)/\sqrt{2}$ is the component of the velocity fluctuation along a line in the x–y plane at 45° to the x-axis. Hence its mean square, $(\boldsymbol{v}_x^2 + \boldsymbol{v}_y^2 + 2\boldsymbol{v}_x\boldsymbol{v}_y)/2$, is the normal stress component over the density in this direction, although it is a combination of normal and tangential stresses in the x- and y-axes.

2.1. Experimental techniques and instrumentation

The recent development of affordable instrumentation such as the Acoustic Doppler Velocimeter (ADV), Acoustic Doppler Current Profiling (ADCP) and the Particle Image Velocity (PIV), has led to an explosion in the number of scientists and engineers conducting 'turbulence' measurements. Unfortunately, some modern instruments have intrinsic weaknesses, and their signal outputs are not always 'true' turbulence measurements. The need for adequate education and training of technicians, engineers, scientists and researchers deploying advanced turbulence equipment in the field and laboratory cannot be overstressed. In this section, the intricacy of turbulent velocity measurements is discussed, using the example of acoustic Doppler velocimetry as an illustration.

In turbulence studies, the sampling duration influences the results, since the turbulence characteristics may be biased with small sample numbers. Basic turbulence studies require large sample sizes: typically 60 000 to 90 000 samples per sampling location.[10,11] Chanson *et al.*[12] recently performed experiments in a large laboratory flume, 0·5 m wide 12 m long, with subcritical and transcritical flow conditions. Turbulent velocity measurements were conducted with a 16 MHz microADV equipped with a two-dimensional side-looking head. Sensitivity analyses were undertaken in steady flows with 25 and 50 Hz sampling rates and total sampling durations between 1 and 60 min, in both gradually varied and uniform equilibrium flows. The results indicated consistently that the statistical properties of the longitudinal velocity, V_x, were most sensitive to the number of data points per sample. The first two statistical moments were adversely affected for sample numbers below 5000 (Fig. 2). Higher statistical moments, such as the skewness and kurtosis, Reynolds stresses and triple correlations,

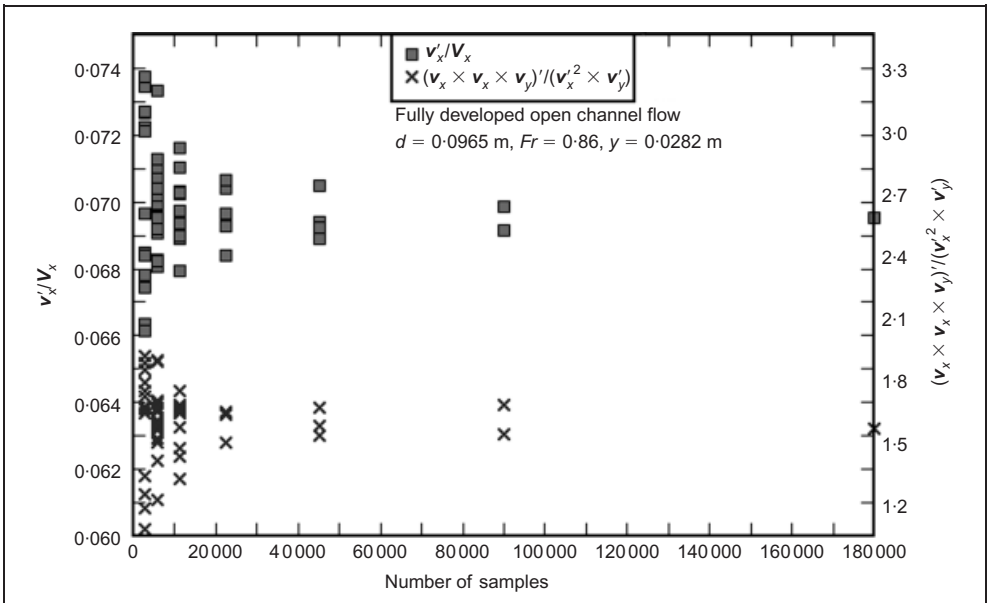

Fig. 2. Effects of sample numbers on turbulence characteristics in a fully developed open channel flow: error on $\boldsymbol{v}'_x/\overline{V}_x$ and $(_x \times \boldsymbol{v}_x \times \boldsymbol{v}_y)'/(\boldsymbol{v}'^2_x \times \boldsymbol{v}'^2_y)$. Flow conditions: $Q = 0{\cdot}0404$ m^3/s, $d = 0{\cdot}096$ m. Micro ADV (16 MHz) with 2D side-looking head: sampling rate 50 Hz, velocity range 1 m/s

were detrimentally influenced for samples numbers less than 25 000 to 50 000 (Fig. 2).

With many velocity probes, the proximity of the sampling volume to a boundary may adversely affect the probe output, especially in small laboratory flumes, for example with the Laser Doppler Velocimeter (LDV), ADV and hot-film probes. Several studies with acoustic Doppler velocimeters have discussed the effects of solid boundary proximity on sampling volume characteristics and the impact on time-averaged velocity data.[12] These findings showed that the streamwise velocity component was underestimated when the solid boundary was less than 30–45 mm from the probe sampling volume. Correction correlations were proposed by Liu *et al.*[13] and Koch and Chanson[14] for micro-ADVs with three-dimensional down-looking and two-dimensional side-looking heads respectively. Chanson *et al.*[12] observed that the effects of wall proximity on the ADV velocity signal were characterised by a significant drop in average signal correlations, in average signal-to-noise ratios and in average signal amplitudes next to the wall. Although Martin *et al.*[15] attributed lower signal correlations to high turbulent shear and velocity gradient across the ADV sampling volume, Chanson *et al.*[12] observed that the decrease in signal-to-noise ratio with decreasing distance from the side wall was the main factor affecting the ADV signal output. It must be stressed that most comparative studies for all probe types have been restricted to limited comparison of the time-averaged streamwise velocity component, and sometimes its standard deviation. No comparative test has been performed to assess velocity probe performance in terms of instantaneous velocities, turbulent velocity fluctuations, Reynolds stresses or other turbulence characteristics. Also, modern velocity measurement techniques (LDV, PIV, ADV) record only the velocity field. Under waves, and in undular flows, the pressure gradient is not hydrostatic, and detailed experiments should record both pressure and velocity fields. In steady flows, the venerable Prandtl–Pitot tube remains the only instrument that can simultaneously record velocity, pressure and total head, and eventually shear stress after a suitable calibration.

Chanson *et al.*[16] and Trevethan *et al.*[17] have presented some high-frequency, long-duration turbulence measurements in a small estuary. Although the acoustic Doppler velocimetry was well suited to the shallow-water flow conditions, all field investigations demonstrated recurrent problems with the velocity data, including large numbers of spikes. Careful analyses of the ADV signal outputs showed that the turbulence properties were inaccurately estimated from the unprocessed ADV signals. 'Classical' despiking methods were not even suitable. A three-stage post-processing method was developed by Chanson *et al.*[16] This technique included an initial velocity signal check, the detection and removal of large disturbances ('pre-filtering'), and the detection and removal of small disturbances ('despiking'). Each stage included velocity error detection and data replacement. The method was successfully applied to long-duration ADV records at high frequency. For all investigations, between 10% and 25% of all samples were deemed erroneous. The findings demonstrated that unprocessed ADV data should not be used to study turbulent flow properties, including time-averaged velocity components.

2.2. Tidal-bore-generated turbulence

A positive surge results from a sudden change in flow that increases the depth. It is the unsteady flow analogy of the stationary hydraulic jump. Positive surges are commonly observed in man-made channels, and a related occurrence is the tidal bore in estuaries (Fig. 3). Most experimental studies have been limited to visual observations and, sometimes, free-surface measurements. Previous studies rarely encompassed turbulence, except for a few limited cases.[14,18]

Figure 4 presents some data on the unsteady turbulent velocity beneath a tidal bore. The measurements were performed in a positive surge with roller ($Fr_1 = 1{\cdot}8$) using acoustic Doppler

Fig. 3. Photograph of the tidal bore of the Sélune river on 7 April 2004

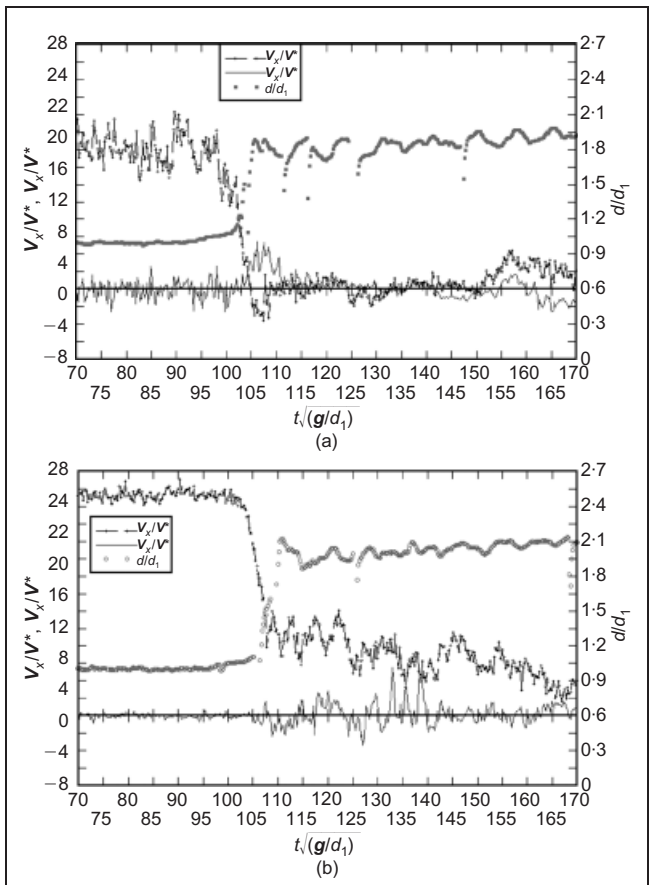

Fig. 4. Instantaneous turbulent velocity measurements V_x/V^* and V_z/V^* beneath a positive surge with roller,[32,34] $d_1 = 0{\cdot}080$ m, $Fr_1 = 1{\cdot}8$, $V^* = 0{\cdot}044$ m/s: (a) $y/d_1 = 0{\cdot}091$ (next to the channel bed); (b) $y/d_1 = 0{\cdot}728$

velocimetry.[14] In Fig. 4 the graphs present the dimensionless velocities V_x/V^* and V_z/V^*, and water depth d/d_1, where V_x is the streamwise velocity, V_z is the transverse horizontal velocity, d_1 is the initial water depth, V^* is the shear velocity measured on the channel centreline in the initially steady flow ($V^* =$ 0·044 m/s) and y is the vertical elevation. The time t was zero at 10 s prior to the surge front passage at the sampling location, and the surge arrival corresponded to $t\sqrt{g/d_1} \approx 90$ (Fig. 4).

The experimental measurements systematically indicated certain basic flow features. The streamwise velocity component decreased rapidly with the passage of the bore front. The sudden increase in water depth yielded a slower flow motion to satisfy conservation of mass. The surge passage was associated with significant fluctuations of the transverse velocity. The velocity records showed some marked differences, depending upon the vertical elevation y (Fig. 4). In the upper flow region ($y/d_1 > 0{\cdot}5$) the longitudinal velocity decreased rapidly at the surge front, although V_x data tended to remain positive beneath the roller toe (Fig. 4(b)). In contrast, next to the bed ($y/d_1 < 0{\cdot}5$) the longitudinal velocity became negative, albeit for a short duration ($104 < t \times \sqrt{g/d_1} < 150$, Fig. 4(a)). The transient flow reversal led to unsteady flow separation.

The instantaneous Reynolds stresses were calculated using a variable-interval time average (VITA) technique, where the cut-off frequency was selected such that the averaging time was greater than the characteristic period of fluctuations, and small with respect to the characteristic period for the time evolution of the mean properties.[9,19] Typical results are shown in Fig. 5, where the instantaneous shear stress data are plotted together with the measured water depth. The experimental data showed large, fluctuating turbulent stresses below the bore front and ensuing flow. The Reynolds stress levels were significantly larger than before the surge passage, and substantial normal and tangential stresses were observed for $y/d_1 > 0{\cdot}5$ (Fig. 5). It is believed that the sudden increase in turbulent stresses was caused by the passage of the developing mixing layer of the roller. In stationary hydraulic jumps and related flows, researchers observed similarly large Reynolds stresses in and next to the developing shear layer.[21–23]

The unsteady turbulence data demonstrated a marked effect of the bore passage (Figs 4 and 5). Longitudinal velocities were characterised by rapid flow deceleration at all vertical elevations, and large fluctuations of transverse velocities were recorded beneath the front (Fig. 4). Turbulent Reynolds stress data highlighted high levels in the lower flow region, including next to the bed, and maximum normal and tangential stresses were observed immediately after the bore front passage (Fig. 5). In a natural channel, bed erosion may take place beneath the surge front, and the eroded material and other scalars are advected in the 'whelps' and wave motion behind the front.

Few field studies have documented the strong turbulent mixing induced by tidal bores in estuarine zones. Unusual mixing patterns have been reported. Kjerfve and Ferreira[24] presented quantitative measurements of salinity and temperature changes behind the tidal bore of Rio Mearim in Brazil. The data showed sharp jumps in salinity and water temperature between 18 and 42 min after the bore passage, depending upon the sampling site location. During one event on 30 January 1991 a 150 kg

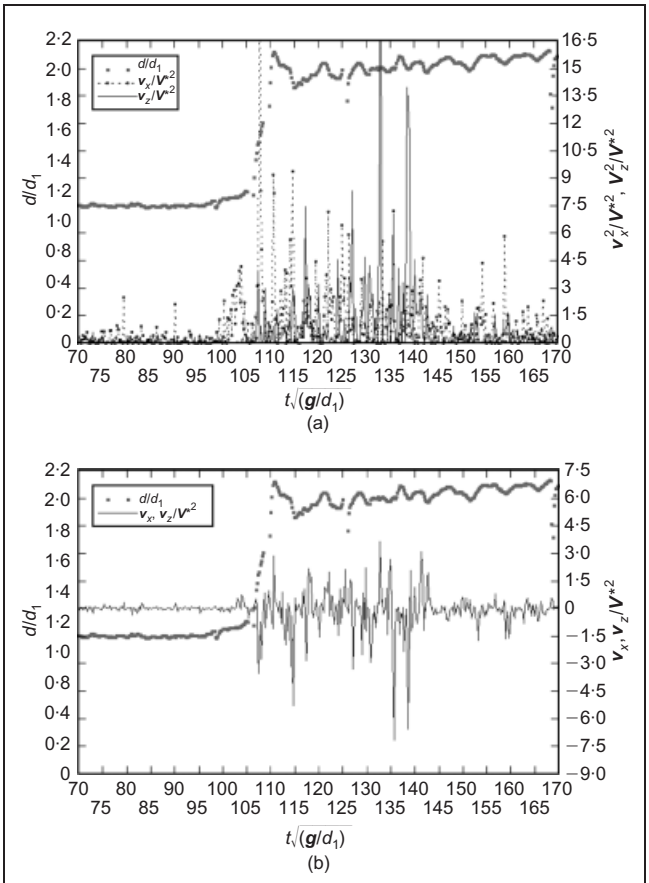

Fig. 5. Turbulent Reynolds stress measurements beneath a positive surge with roller,[14,20] $d_1 = 0{\cdot}080$ m, $Fr_1 = 1{\cdot}8$, $V^* = 0{\cdot}044$ m/s: (a) normal stresses v_x^2/V^*2 and v_z^2/V^*2 at $y/d_1 = 0{\cdot}728$; (b) tangential stress $v_x v_z/V^*2$ at $y/d_1 = 0{\cdot}728$

sawhorse was toppled down, tumbled for 1·4 km and was buried deep in sand. Wolanski *et al.*[25] studied the Daly river bore in Australia at a site located 30–40 km upstream of the river mouth. On 2 July 2003 a period of strong turbulence was observed for about 3 min, about 20 min after the bore passage. During this 'turbulence patch', a tripod holding instruments was knocked down. Further field evidences encompassed repeated impact and damage to field measurement equipment in Rio Mearim, in the Daly river, and in the Dee river in the UK; other demonstrations included major damage to river banks and navigation, as well as numerous drownings in tidal bore 'whelps' in the Seine (France), Qiantang (China) and Colorado (Mexico) rivers.

3. INTERACTIONS BETWEEN OPEN CHANNEL FLOW AND ITS SURROUNDINGS

Natural channels have the ability to scour channel bed and banks, to carry sediment materials, and to deposit sediment load. For example, during a flood event, the Yellow River eroded its bed by 7 m in less than 60 h at Longmen, in the middle reach of the river, with a peak discharge of 7460 m^3/s in July 1966.[26] Traditional fixed-boundary fluid dynamics cannot predict the morphological changes of natural streams because of the numerous interactions with the catchment, its hydrology and the sediment transport processes.

In nature, air–water flows highlight another form of interaction between turbulent flow motion and its

surroundings. In turbulent free-surface flows, air bubbles may be entrained when the turbulent kinetic energy is large enough to overcome both surface tension and gravity effects. The process is also called 'white water'. Through the free surface there are continuous exchanges of both mass and momentum between the water and the atmosphere. Air–water mixing is an important reoxygenation process, because the entrainment of air bubbles dramatically increases the area of the air–water interface, and hence the air–water transfer rate.[27] In spillway design, free-surface aeration may affect the thickness of flowing water and hence side wall design. The presence of air bubbles in shear flows may reduce the shear stress between flow layers, and induce some drag reduction. It may also prevent or reduce the damage caused by cavitation.[28]

The interactions between open channel flow and its surroundings remain a key challenge. Two applications are discussed in the following paragraphs: rapid reservoir siltation resulting from sediment trapping, and air entrainment in high-velocity flows.

3.1. Extreme reservoir siltation

When a dam is built across a river, its wall acts as a sediment trap. After several years, the reservoir can become filled with sediments, and cease to provide adequate water storage. The primary consequence is a reduction of the reservoir's capacity, leading to economic and strategic losses. Fig. 6 presents some examples of rapid siltation. In each case the reservoir failed because the designers did not understand the basic concepts of soil erosion, sediment transport and catchment management. Reservoir sedimentation is a very complex process. The dam, the reservoir and the catchment must be analysed as a complete system; they cannot be dissociated. One issue is the lack of acknowledgement of sedimentation problems: for example, in Australia the issue of reservoir siltation was ignored and rejected until the 1980s.[29,30]

A proper understanding of reservoir siltation mechanics requires a broad knowledge of all the intervening parameters, including long-term climatic changes. The world community has focused its attention on the early detection of El Niño, which is termed a 'major catastrophe' in Australia. (El Niño is associated with very long periods of drought in eastern Australia.) Interestingly, inter-annual climatic events associated with long periods of drought were first established between 1878 and 1888 by Sir Charles Todd, South Australia Government Observer, and were well documented by H. C. Russell, New South Wales Government Observer.[31] The El Niño Southern Oscillation (ENSO) phenomenon is a recurrent climate pattern with an average period of about five to seven years. In Australia, the drought period ends with a series of intense rainfall events during the La Niña event, and there is a strong correlation between extreme siltation events and La Niña events.[29] Examples include the Junction Reefs reservoir (1902 floods after the Great Drought of 1900–1902), the Moore Creek reservoir (flood of February 1908), the Gap weir (floods of 1919), the Melton reservoir (flood of 1941), and the Quipolly reservoir (floods of 1942–43). However, the El Niño/La Niña phenomena are not properly managed by local, national or international institutions,[32] and there is an absence of long-term policy to deal with the impact of the ENSO climatic pattern on reservoir management.

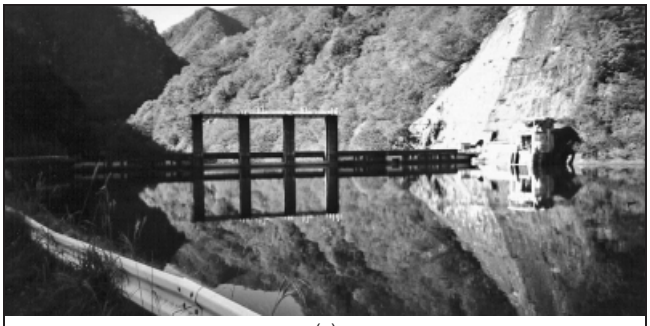

(a)

(b)

Fig. 6. Extreme reservoir siltation. (a) Nishiyawa dam on the Hayakawa river (Japan, 1957), looking at the dam wall in November 1998. Dam: $H = 39$ m, $L = 112$ m. Reservoir capacity: 2·38 M.m^3. Spillway capacity $\boldsymbol{Q} = 575$ m^3/s. Reservoir fully silted by gravel bed-load in less than 20 years, and dredged around 1988 to resume hydropower operation. (b) Fully silted debris dam upstream of the Saignon dam reservoir, La Motte-du-Caire (France, 1961) in June 1998. Despite several debris dams, the Saignon reservoir (dam: $H = 14·5$ m, reservoir capacity 0·14 M.m^3, catchment area 3·5 km^2) became itself fully silted in only two years

Reservoir siltation is a major global issue, and progress must be linked with advances in soil conservation, while management practices are required. Very little is known about soil erosion by rainfall droplets, the impact of forestation on sediment runoff, or the effects of rural practices, although major soil conservation programmes were successfully undertaken in Austria, France (Grands Travaux de Forestation) and Japan

around 1850–1930.[33] A major engineering challenge is the development of efficient desilting devices. Current sediment flushing systems are not very different from those introduced by the Nabataeans, Romans and Spaniards many centuries ago.

3.2. Air entrainment in hydraulic engineering

Air entrainment is defined as the entrapment of air bubbles that are advected within the turbulent flow (Fig. 7). The entrainment of air pockets can be localised or continuous along the air–water interface (Fig. 8). Examples of localised aeration include air entrainment by a plunging jet and at a hydraulic jump. Bubbles are entrained locally at the intersection of the impinging jet with the surrounding waters (Fig. 8(b)). The intersecting perimeter is a singularity in terms of both air entrainment and momentum exchange, and the air is entrapped at the discontinuity between the impinging jet flow and the receiving pool of water. Interfacial aeration is defined as the air entrainment process along an air–water interface, usually parallel to the flow direction (Fig. 8(a)).

Air–water flows have been studied only relatively recently. The first successful experiments were conducted during the 1920s and 1950s.[34,35] A milestone contribution was the series of experiments performed on the Aviemore dam spillway in New Zealand.[36,37] Both laboratory and prototype investigations showed the complexity of the free-surface aeration process, and some recent studies have highlighted the strong interactions between entrained bubbles and turbulence.[38–40] These significant findings are incomplete. For example, there are still some fundamental reservations about the extrapolation of laboratory results to a full-size prototype, as shown in Fig. 7.[41]

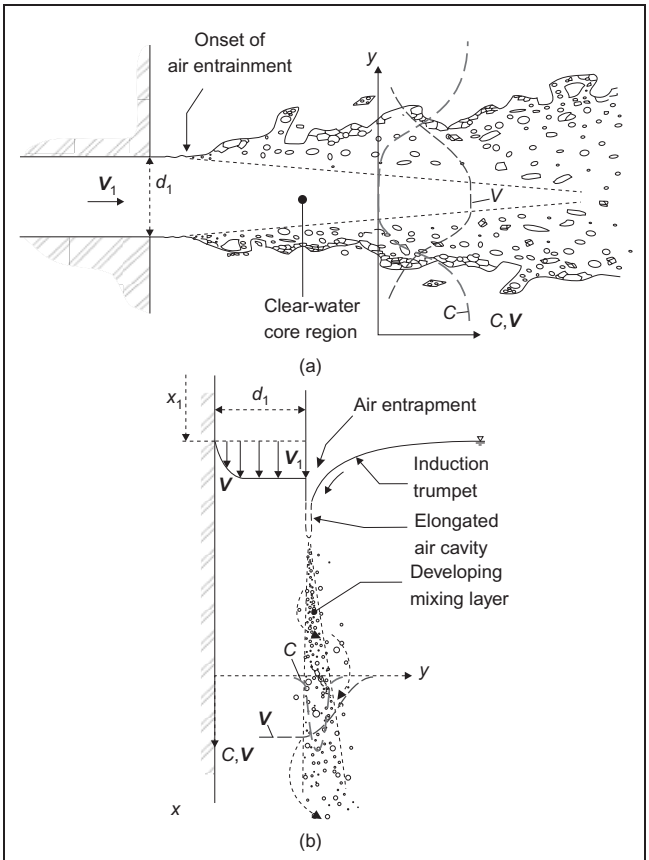

Fig. 8. Definition sketches of interfacial and singular air bubble entrainment: (a) interfacial aeration in a water jet discharging into atmosphere; (b) singular aeration at a vertical two-dimensional plunging jet

The onset of air entrainment is defined as a threshold situation above which air entrainment takes place. While there is some distinction between the first bubble entrapment and the start of continuous air bubble entrainment, the corresponding flow conditions usually fall within a very narrow range, called the onset conditions. Early studies expressed the inception conditions as functions of a time-averaged velocity. For example, air entrainment in turbulent water flows occurs when the flow velocity exceeds roughly 0·5–2 m/s. The approach does not account for the complexity of the flow, nor for the turbulence properties. Recent studies have linked the onset of air entrainment with a characteristic level of normal Reynolds stresses next to the free surface: for example Ervine and Falvey[42] and Chanson[43] for water jets and steep chute flows, Cummings and Chanson[44] for plunging jets, Brocchini and Peregrine,[38] and Chanson.[45] A summary of experimental results for vertical plunging water jets is presented in Fig. 9. This shows the dimensionless onset velocity $\mu_w V/\sigma$ as a function of the dimensionless normal turbulent stress v'^2/V^2, where V is the jet velocity at impingement, v' is the root mean square of the jet velocity, μ_w is the water dynamic viscosity, and σ is the surface tension between air and water. All the data collapse into a well-defined trendline.

Fig. 7. Air entrainment in hydraulic engineering. Free-surface aeration at bottom and sluice outlets of Three Gorges Dam on 20 October 2004: $V_1 = 35$ m/s, $H = 70$ m

The inception of air entrainment is linked to a characteristic level of tangential Reynolds stresses next to the free surface. Experimental evidence shows that the free-surface of turbulent flows exhibits surface waves with a fine-grained turbulent structure and larger underlying eddies. Since the turbulent energy is high in small eddy lengths close to the free surface, air bubble entrainment may result from the action of high-intensity turbulent shear close to the air–water interface. Free-surface break-up and bubble entrapment occur when the turbulent shear stress is greater than the capillary force per unit area resisting the surface break-up. The onset condition is defined by

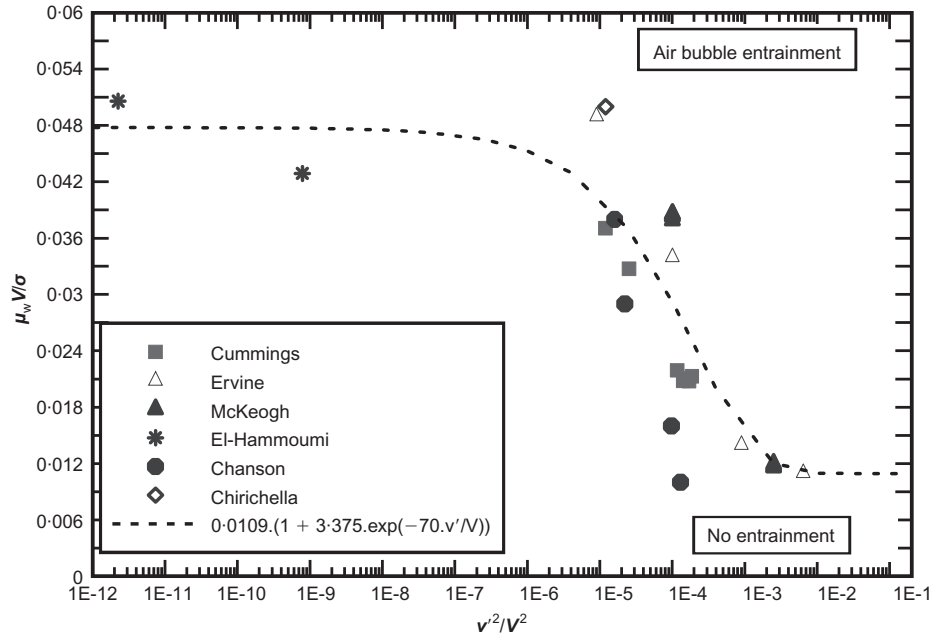

Fig. 9. Onset of air bubble entrainment in vertical plunging jets. Two-dimensional supported jet data: Cummings and Chanson.[44] Circular jet data: McKeogh,[46] Ervine *et al.*,[47] El-Hammoumi,[48] Chirichella *et al.*[49] and Chanson and Manasseh[50]

$$|\rho_w \boldsymbol{v}_i \boldsymbol{v}_j| > \boldsymbol{\sigma} \frac{\pi(r_1 + r_2)}{A} \quad (1)$$

where ρ_w is the water density; $\boldsymbol{v}$ is the instantaneous turbulent velocity fluctuation; (i, j) is the directional tensor ($i, j = x, y, z$); $\pi(r_1 + r_2)$ is the perimeter along which surface tension acts; r_1 and r_2 are the two principal radii of curvature of the free-surface deformation; and A is the surface deformation area. Equation (1) gives a criterion for the onset of free-surface aeration in terms of the magnitude of the instantaneous tangential Reynolds stress, the air/water physical properties, and the free-surface deformation properties. Air bubbles cannot be entrained across the free surface until there is sufficient tangential shear relative to the surface tension force per unit area.

For a three-dimensional flow with quasi-isotropic turbulence, the smallest interfacial area per unit volume of air is the sphere (radius r), and equation (1) gives a condition for the onset of spherical bubble entrainment

$$|\rho_w \boldsymbol{v}_i \boldsymbol{v}_j| > \frac{\boldsymbol{\sigma}}{2\pi r} \quad (2)$$

Equation (2) implies that the onset of air bubble entrainment takes place predominantly in the form of relatively large bubbles. However, the largest bubbles are detrained by buoyancy, and this yields some preferential size of entrained bubbles, observed to be about 1–100 mm in prototype turbulent flows.[27,36,43]

Once entrained, the air bubbles are advected in a turbulent shear flow, where the entrained air is broken into small bubbles. In an equilibrium situation, a maximum bubble size may be estimated by the balance between the surface tension force and the inertial force caused by the velocity changes over distances of the order of the bubble size.[51] The result is limited, however, because equilibrium situations are rare, and it is simply not applicable in many turbulent shear flows.

In turbulent air–water flows, experimental observations imply that the air bubble sizes are larger than the Kolmogorov microscale and smaller than the turbulent macroscale.[27] This suggests that the length scale of the vortices responsible for breaking up the bubbles is close to the bubble size. Larger eddies advect the bubbles, whereas eddies with length scales substantially smaller than the bubble size do not have the required energy to break up the bubbles. In a shear flow, bubble break-up occurs when the tangential shear stress is greater than the capillary force per unit area. For an elongated spheroid, bubble break-up takes place for

$$|\rho_w \boldsymbol{v}_i \boldsymbol{v}_j| > \boldsymbol{\sigma} \frac{\pi(r_1 + r_2)}{2\pi r_1 \left\{ r_1 + r_2 \dfrac{\arcsin\left[\sqrt{1 - (r_1^2/r_2^2)}\right]}{\sqrt{1 - (r_1^2/r_2^2)}} \right\}} \quad (3)$$

where r_1 and r_2 are the equatorial and polar radii of the ellipsoid respectively, with $r_2 > r_1$. Equation (3) implies that some turbulence anisotropy (e.g. $\boldsymbol{v}_x, \gg \boldsymbol{v}_y, \boldsymbol{v}_z$) must induce some preferential bubble shapes and sizes.

4. CONCLUSION

Hydraulic engineers and researchers deal with many scientific challenges involving turbulent flow motion and the interactions with the surroundings (movable bed, free surface, aquatic life). Turbulent flows are characterised by unpredictable behaviour associated with strong turbulent mixing. With recent developments in affordable instrumentations, many scientists

and engineers have undertaken 'turbulence measurements', but without adequate education, training, and expertise. Many modern instruments have intrinsic weaknesses that adversely affect the quality of the signal outputs. Some experience with acoustic Doppler velocimetry is illustrated. A challenging environmental application is the tidal bore, and the understanding of unsteady turbulence beneath a propagating surge is essential to comprehend the basic sediment transport processes.

The interactions between an open channel flow and its surroundings remain a key challenge. Two examples illustrate our limited knowledge: rapid reservoir siltation, and air entrainment in turbulent free-surface flows. In both applications, hydraulic engineers require basic expertise in hydrodynamics, turbulence, multiphase flows, and geomorphology. The education of these hydraulic engineers is a challenge for present and future generations. Although some introductory courses are offered at undergraduate level, most hydraulic engineering subjects are offered at postgraduate level only, and they rarely encompass the complex interactions between water, soil, air and aquatic life.

REFERENCES

1. BURDY J. *Préinventaire des Monuments et Richesses Artistiques. IV Lyon. L'Aqueduc Romain du Gier*. Bosc Frères, Lyon, 1996.
2. BURDY J. *Les Aqueducs Romains de Lyon*. Presses Universitaires de Lyon, Lyon, 2002.
3. HODGE A. T. *Roman Aqueducts and Water Supply*, 2nd edn. Duckworth, London, 2002.
4. SMITH N. A. F. The hydraulics of ancient pipes and pipelines. *Transactions of the Newcomen Society*, 2007, **77**, No. 1, 1–49.
5. HERSCHY R. The world's maximum observed floods. *Flow Measurement and Instrumentation*, 2002, **13**, 231–235.
6. REYNOLDS O. An experimental investigation of the circumstances which determine whether the motion of water shall be direct or sinuous, and the laws of resistance in parallel channels. *Philosophical Transactions of the Royal Society of London*, 1883, **174**, 935–982.
7. REYNOLDS O. *On Certain Laws Relating to the Regime of Rivers and Estuaries, and on the Possibility of Experiments on a Small Scale*. British Association Report, UK 1887.
8. BRADSHAW P. *An Introduction to Turbulence and its Measurement*. Pergamon Press, Oxford, 1971, p. 17.
9. PIQUET J. *Turbulent Flows: Models and Physics*. Springer, Berlin, 1999.
10. KARLSSON R. I. and JOHANSSON T. G. LDV measurements of higher order moments of velocity fluctuations in a turbulent boundary layer. *Proceedings of the 3rd International Symposium on Applications of Laser Anemometry to Fluid Mechanics, Lisbon*, 1986, 276–289.
11. KROGSTAD P. A., ANDERSSON H. I., BAKKEN O. M. and ASHRAFIAN A. A. An experimental and numerical study of channel flow with rough walls. *Journal of Fluid Mechanics*, 2005, **530**, 327–352.
12. CHANSON H., TREVETHAN M. and KOCH C. Turbulence measurements with acoustic Doppler velocimeters. *Journal of Hydraulic Engineering, ASCE*, 2007, **133**, No. 11, 1283–1286.
13. LIU M., ZHU D. and RAJARATNAM N. Evaluation of ADV measurements in bubbly two-phase flows. *Proceedings of the Conference on Hydraulic Measurements and Experimental Methods*, Estes Park, USA, 2002, 10 pp. (CD-ROM).
14. KOCH C. and CHANSON H. *An Experimental Study of Tidal Bores and Positive Surges: Hydrodynamics and Turbulence of the Bore Front*. Department of Civil Engineering, University of Queensland, Brisbane, 2005, Report No. CH56/05.
15. MARTIN V., FISHER T. S. R., MILLAR R. G. and QUICK M. C. ADV data analysis for turbulent flows: low correlation problem. *Proceedings of the Conference on Hydraulic Measurements and Experimental Methods*, Estes Park, USA, 2002, 10 pp. (CD-ROM).
16. CHANSON H., TREVETHAN M. and AOKI S. Acoustic Doppler velocimetry (adv) in a small estuarine system: field experience and 'despiking'. *Proceedings of the 31st Biennial IAHR Congress, Seoul*, 2005, 3954–3966.
17. TREVETHAN M., CHANSON H. and TAKEUCHI M. Continuous high-frequency turbulence and sediment concentration measurements in an upper estuary. *Estuarine Coastal and Shelf Science*, 2007, **73**, No. 1–2, 341–350.
18. HORNUNG H. G., WILLERT C. and TURNER S. The flow field downstream of a hydraulic jump. *Journal of Fluid Mechanics*, 1995, **287**, 299–316.
19. KOCH C. and CHANSON H. Unsteady turbulence characteristics in an undular bore. *Proceedings of the International Conference on Fluvial Hydraulics of River Flow* (FERREIRA R. M. L., ALVES E. C. T. L., LEAL J. G. A. B. and CARDOSO A. H. (eds)). Balkema, London, 2006, Vol. 1, pp. 79–88.
20. KOCH C. and CHANSON H. Turbulence measurements in positive surges and bores. *Journal of Hydraulic Research*, IAHR, 2008, **46** (in press).
21. LIU M. *Turbulence Structure in Hydraulic Jumps and Vertical Slot Fishways*. PhD thesis, Department of Civil and Environmental Engineering, University of Alberta, Edmonton, Canada, 2004.
22. MURZYN F. and CHANSON H. *Free Surface, Bubbly Flow and Turbulence Measurements in Hydraulic Jumps*. Division of Civil Engineering, University of Queensland, Brisbane, 2007, Report No. CH63/07.
23. RESCH F. J. and LEUTHEUSSER H. J. Reynolds stress measurements in hydraulic jumps. *Journal of Hydraulic Research*, 1972, **10**, No. 4, 409–429.
24. KJERFVE B. and FERREIRA H. O. Tidal bores: first ever measurements. *Ciência e Cultura (Journal of the Brazilian Association for the Advancement of Science)*, 1993, **45**, No. 2, 135–138.
25. WOLANSKI E., WILLIAMS D., SPAGNOL S. and CHANSON H. Undular tidal bore dynamics in the Daly Estuary, Northern Australia. *Estuarine, Coastal and Shelf Science*, 2004, **60**, No. 4, 629–636.
26. WAN Z. and WANG Z. *Hyperconcentrated Flow*. IAHR Monograph. Balkema, Rotterdam, 1994.
27. CHANSON H. *Air Bubble Entrainment in Free-Surface Turbulent Shear Flows*. Academic Press, London, 1997.
28. WOOD I. R. Air entrainment in free-surface flows. In *IAHR Hydraulic Structures Design Manual No. 4: Hydraulic Design Considerations*. Balkema, Rotterdam, 1991.
29. CHANSON H. and JAMES D. P. Teaching case studies in reservoir siltation and catchment erosion. *International*

Journal of Engineering Education, 1998, **14**, No. 4, 265–275.
30. CHANSON H. and JAMES D. P. Siltation of Australian reservoirs: some observations and dam safety implications. *Proceedings of the 28th IAHR Biennial Congress, Graz*, 1999, Session B5, 6 pp. (CD-ROM).
31. GROVE R. H. The East India Company, the Australians and the El-Niño: colonial scientists and analysis of the mechanisms of global climatic change and teleconnections between 1770 and 1930. *Working Papers in Economic History*, Australian National University, Canberra, 1995, Working Paper No. 182.
32. SCHUBERT S., KOSTER R., HOERLING M., SEAGER R., LETTENMAIER D., KUMAR A. and GUTZLER D. Predicting drought on seasonal-to-decadal time scales. *Bulletin of the American Meteorological Society*, 2007, **88**, No. 10, 1625–1630.
33. CEMAGREF. *L'Etude de l'Erosion des Marnes: les Bassins Versants Expérimentaux de Draix. Etude et Mesure de l'Erosion. Présentation et Synthèse*, 2nd edn. CEMAGREF, Aix-en-Provence, 1988.
34. EHRENBERGER R. Wasserbewegung in steilen Rinnen (Susstennen) mit besonderer Berucksichtigung der Selbstbelüftung. *Zeitschrift des Österreichischer Ingenieur und Architektverein*, 1926, No. 15/16, 17/18.
35. STRAUB L. G. and ANDERSON A. G. Experiments on self-aerated flow in open channels. *Journal of the Hydraulics Division, ASCE*, 1958, **84**, No. HY7, pp. 1890-1–1890-35.
36. CAIN P. *Measurements within Self-Aerated Flow on a Large Spillway*. PhD thesis, Department of Civil Engineering, University of Canterbury, Christchurch, New Zealand, 1978.
37. CAIN P. and WOOD I. R. Measurements of self-aerated flow on a spillway. *Journal of the Hydraulics Division, ASCE*, 1981, **107**, No. HY11, 1425–1444.
38. BROCCHINI M. and PEREGRINE D. H. The dynamics of strong turbulence at free surfaces. Part 2. Free-surface boundary conditions. *Journal of Fluid Mechanics*, 2001, **449**, 255–290.
39. CHANSON H. and CAROSI G. Turbulent time and length scale measurements in high-velocity open channel flows. *Experiments in Fluids*, 2007, **42**, No. 3, 385–401.
40. CHANSON H. and TOOMBES L. Air–water flows down stepped chutes: turbulence and flow structure observations. *International Journal of Multiphase Flow*, 2002, **28**, No. 11, 1737–1761.
41. CHANSON H. Air entrainment in hydraulic engineering. In *Fluvial, Environmental and Coastal Developments in Hydraulic Engineering* (MOSSA M., YASUDA Y. and CHANSON H. (eds)). Balkema, Leiden, 2004, pp. 17–63.
42. ERVINE D. A. and FALVEY H. T. Behaviour of turbulent water jets in the atmosphere and in plunge pools. *Proceedings of the Institution of Civil Engineers, Part 2*, 1987, **83**, No. 1, 295–314.
43. CHANSON H. Self-aerated flows on chutes and spillways. *Journal of Hydraulic Engineering, ASCE*, 1993, **119**, No. 2, 220–243.
44. CUMMINGS P. D. and CHANSON H. An experimental study of individual air bubble entrainment at a planar plunging jet. *Chemical Engineering Research and Design*, 1999, **77**, No. A2, 159–164.
45. CHANSON H. Advective diffusion of air bubbles in turbulent water flows. In *Fluid Mechanics of Environmental Interfaces* (GUALTIERI C. and MIHAILOVIC D. T. (eds)). Taylor & Francis, Leiden, 2008, pp. 163–196.
46. MCKEOGH E. J. *A Study of Air Entrainment using Plunging Water Jets*. PhD thesis, Queen's University of Belfast, UK, 1978.
47. ERVINE D. A., MCKEOGH E. J. and ELSAWY E. M. Effect of turbulence intensity on the rate of air entrainment by plunging water jets. *Proceedings of the Institution of Civil Engineers, Part 2*, 1980, **69**, No. 2, 425–445.
48. EL HAMMOUMI M. *Entraînement d'Air par Jet Plongeant Vertical. Application aux Becs de Remplissage pour le Dosage Pondéral*. PhD thesis, INPG, Grenoble, France, 1994.
49. CHIRICEILLA R., GOMEZ LEDESMA R., KIGER K. T. and DUNCAN H. Incipient air entrainment in a translating axisymmetric plunging laminar jet. *Physics of Fluids*, 2002, **14**, No. 2, 781–790.
50. CHANSON H. and MANASSEH R. Air entrainment processes in a circular plunging jet: void fraction and acoustic measurements. *Journal of Fluids Engineering, ASME*, 2003, **125**, No. 5, 910–921.
51. HINZE J. O. Fundamentals of the hydrodynamic mechanism of splitting in dispersion processes. *Journal of the American Institute of Chemical Engineers*, 1955, **1**, No. 3, 289–295.